



Aalborg Universitet

AALBORG UNIVERSITY
DENMARK

Compliance and Fatigue Life Analysis of U-shaped Flexure Hinge

Liang, Jingjing; Li, Ruiqin; Bai, Shaoping; Li, Qing; NING, Fengping ; KANG, Shuhua

Published in:
Mechanika

DOI (link to publication from Publisher):
[10.5755/j01.mech.25.6.22686](https://doi.org/10.5755/j01.mech.25.6.22686)

Creative Commons License
CC BY 4.0

Publication date:
2019

Document Version
Publisher's PDF, also known as Version of record

[Link to publication from Aalborg University](#)

Citation for published version (APA):
Liang, J., Li, R., Bai, S., Li, Q., NING, F., & KANG, S. (2019). Compliance and Fatigue Life Analysis of U-shaped Flexure Hinge. *Mechanika*, 25(6). <https://doi.org/10.5755/j01.mech.25.6.22686>

General rights

Copyright and moral rights for the publications made accessible in the public portal are retained by the authors and/or other copyright owners and it is a condition of accessing publications that users recognise and abide by the legal requirements associated with these rights.

- Users may download and print one copy of any publication from the public portal for the purpose of private study or research.
- You may not further distribute the material or use it for any profit-making activity or commercial gain
- You may freely distribute the URL identifying the publication in the public portal -

Take down policy

If you believe that this document breaches copyright please contact us at vbn@aub.aau.dk providing details, and we will remove access to the work immediately and investigate your claim.

Compliance and Fatigue Life Analysis of U-shape Flexure Hinge

Jingjing LIANG*, Ruiqin LI*, Shaoping BAI**, Qing LI*, Fengping NING*, Shuhua KANG*

*School of Mechanical Engineering, North University of China, Taiyuan, China, 03005,
E-mail: liruiqin@nuc.edu.cn (Corresponding author)

**Department of Mechanical and Manufacturing Engineering, Aalborg University, 9220 Aalborg, Denmark,
E-mail: shb@mp.aau.dk

crossref <http://dx.doi.org/10.5755/j01.mech.25.6.22686>

1. Introduction

The flexure hinge is a kind of special kinematic pair which makes use of the deformation of materials to provide finite angular displacement of complex movement around central axis. Compared with the traditional rigid structure, the flexure hinge has no friction, no abrasion, no clearance, low noise, small space size. The flexure hinge can be designed and fabricated in one body, which can realize high precision motion. The compliance can be used to protect the mechanism against impact amongst many other advantages. Flexure hinges are extensively applied in various fields requiring ultra-precision positioning, micromanipulation, microelectronics, and micro assembly for optoelectronic components, optics, bioengineering, and many other fields [1-3].

Up to date, researches on flexure hinge are mainly focused on the notch flexure hinge, reed flexure hinge, as well as flexible elements, such as rods, reeds, and the combination of flexure hinges with different notch shapes. The notch flexure hinge has higher precision but a smaller range of movement, which is more suitable for micro-displacement application. The reed flexure hinge has a larger rotation angle, but lower rotation accuracy. The combined hinge has better comprehensive performance [4-11].

Extensive researches on flexure hinges have been reported. Tian et al. proposed a V-type hinge structure, for which the compliance and rotation precision characteristics were analyzed by finite element method [12]. Chen et al. obtained two generalized models that are the conic model and the elliptic-arc-fillet model by using the ratio of the radius of curvature of the stress-concentrating feature to the minimum thickness as the only fitting variable [13]. Xu et al. presented analytic models of four types of flexure hinges: elliptic, circular, parabolic, and hyperbolic. These analytic models are developed based on the theory of elasticity and infinitesimal method, and devoted a hinge index by the ratio of rotational precision and rotational stiffness, to estimate the mechanical properties of diverse flexure hinges synthetically and quantitatively [14]. Li et al. developed a generalized analytical compliance model that can quickly formulate the equations of compliance and precision for hybrid flexure hinges [15]. Wang et al. presented the development of a parametric model for the rotational compliance of a cracked right circular flexure hinge. The rotational compliance of the cracked right circular flexure hinge was obtained from the sum of the rotational compliance of a healthy flexure hinge and the change of the rotational compliance due to the crack [16]. Li et al. presented a new type power-function-shaped

flexure hinge, derived the closed-form compliance equations of the flexure hinge based on the unit-load method, and investigated the motion accuracy [17]. Meng et al. investigated the existing stiffness equations for corner-filletted flexure hinges. Three empirical stiffness equations for corner-filletted flexure hinges were formulated based on finite element analysis [18]. Li et al. derived empirical compliance equations for circular flexure hinge considering the effect of stress concentration [19].

The notch flexure hinge is mostly applied to micro-operation robots, magnifying mechanism for micrometric displacement, and compliance straight-line guidance mechanism, which has simple structure and can be processed as a whole. A thorough review of flexure hinges has indicated that different notch shape flexure hinges have been utilized to improve the performance. This paper presents a U-shape flexure hinge with four structures and the compliance equations for the flexure hinges. The influences of the structure parameters on the performance of these types of flexure hinges are investigated. It is found that the U-shape flexure hinges have a large compliance ranges corresponding to different notch size. This makes such flexure hinges capable of being used in wide potential applications with different requirements. The finite element analysis is used to comparing fatigue life of U-shape flexure hinges and circular flexure hinge, which reveals a longer fatigue life with U-shape design.

2. Compliance analysis

The U-shape flexure hinges are shown in Fig. 1, where four structural forms are displayed. In the flexures, notches are constructed with elliptic arc or circular arc connected by straight line segments.

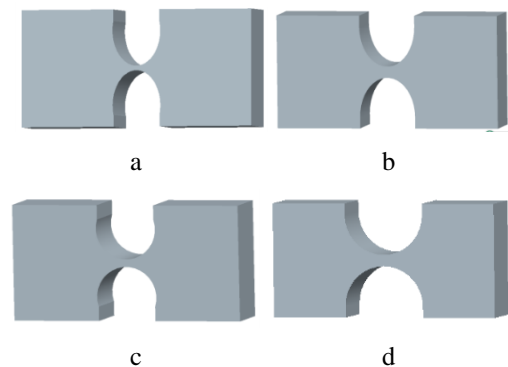


Fig. 1 Four kinds of U-shape flexure hinges with different structures: a – $a \neq b$ and $2b > m$; b – $a \neq b$ and $2b = m$; c – $a = b$ and $2b > m$; d – $a = b$ and $2b = m$

The structure parameters of the flexure hinge are shown in Fig. 2, including:

- the opening width m ;
- the opening depth n of straight-line segments;
- the semi major axis a and semi minor axis b of the ellipse;
- the minimum thickness t of the flexure hinge center;
- the length L , width W and height H of the flexure hinge.

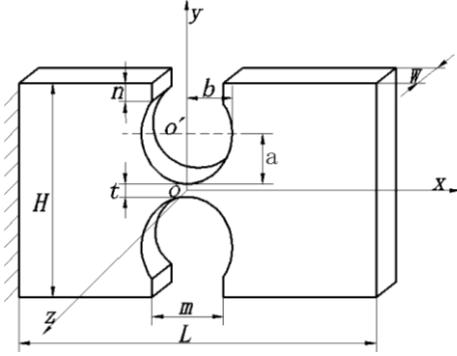


Fig. 2 Structural parameters of a U-shape flexure hinge

The compliance of the flexure hinges is mainly determined by the material and structural parameters. Thus, it is necessary to establish the relations between the compliance and structural parameters of the flexure hinge and reveal the influence of the structural parameters on the compliance to provide the theoretical basis for such engineering design and optimization of the flexure hinge. In the engineering application, the flexure hinge can have micro deformations in the displacement and the angle under the external load. In the analysis of compliance, it is assumed that the left end of the flexure hinge (being fixed) and the right end (being free) are each under the influence of the axial force F_x ; shear forces F_y, F_z ; and bending moments M_y, M_z as shown in Fig. 3. The coordinate system O - xyz is established with the geometric center of the hinge as the coordinate origin O .

The flexure hinge is subject to the above loads. According to Castigliano's second theorem [20]:

$$\delta_i = \frac{\partial V_\varepsilon}{\partial F_i}, \quad (1)$$

where: δ_i is displacement corresponding to force F_i , V_ε is structural deformation energy, F_i is generalized force.

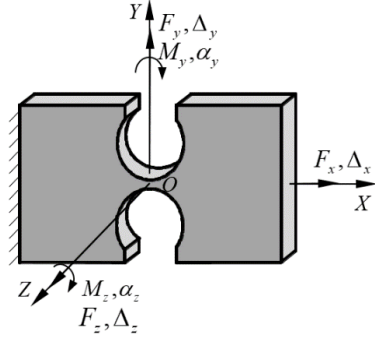


Fig. 3 The loads applied to U-shape flexure hinge

If F_i is axial tension pressure, Eq. (1) becomes:

$$\delta_i = \frac{\partial V_\varepsilon}{\partial F_i} = \frac{\partial}{\partial F_i} \int \frac{F_N^2(x)}{2EA} dx, \quad (2)$$

where: F_N is axial force, E is modulus of elasticity, and A is cross sectional area.

Otherwise, if F_i is the bending moment, Eq. (1) is:

$$\delta_i = \frac{\partial V_\varepsilon}{\partial F_i} = \frac{\partial}{\partial F_i} \int \frac{M^2(x)}{2EI} dx, \quad (3)$$

where: M is bending moment, and I is area moment of inertia.

A flexure hinge will generate five kinds of displacements, namely, linear displacements x, y, z and angular displacements α_y, α_z respectively, which can be obtained based on the theory of material mechanics about load-bearing and deformation relations as follows:

$$\begin{bmatrix} x \\ y \\ z \\ \alpha_y \\ \alpha_z \end{bmatrix} = \begin{bmatrix} C_{x-F_x} & 0 & 0 & 0 & 0 \\ 0 & C_{y-F_y} & 0 & 0 & C_{y-M_z} \\ 0 & 0 & C_{z-F_z} & C_{z-M_y} & 0 \\ 0 & 0 & C_{\alpha_y-F_z} & C_{\alpha_y-M_y} & 0 \\ 0 & C_{\alpha_z-F_y} & 0 & 0 & C_{\alpha_z-M_z} \end{bmatrix} \begin{bmatrix} F_x \\ F_y \\ F_z \\ M_y \\ M_z \end{bmatrix}. \quad (4)$$

For the convenience of analysis and calculation, region segmentation has been made for the notch part of the flexure hinge, as shown in Fig. 4.

In Fig. 4, lengths l_A , l_B and l_C are calculated by:

$$l_A(x) = 2a - 2a \cos \phi + t,$$

$$dx = b \cos \phi d\phi, \quad \phi \in \left[-\frac{\pi}{2}, \frac{\pi}{2} \right],$$

$$l_B(x) = 2[n + a \cos \phi_0 - a \cos \phi],$$

$$dx = b \cos \phi d\phi, \quad \phi \in \left[-\frac{\pi}{2}, -\phi_0 \right],$$

$$l_C(x) = 2[n + a \cos \phi_0 - a \cos \phi],$$

$$dx = b \cos \phi d\phi, \quad \phi \in \left[\phi_0, \frac{\pi}{2} \right].$$

$$\text{Let } \frac{a}{t} = p, \quad s(\phi) = 2p - 2p \cos \phi + 1, \quad \frac{a}{n} = q,$$

$$k(\phi) = 1 + q \cos \phi_0 - q \cos \phi,$$

then: $l_A(x) = t \cdot s(\phi)$, $l_B(x) = l_C(x) = 2n \cdot k(\phi)$.

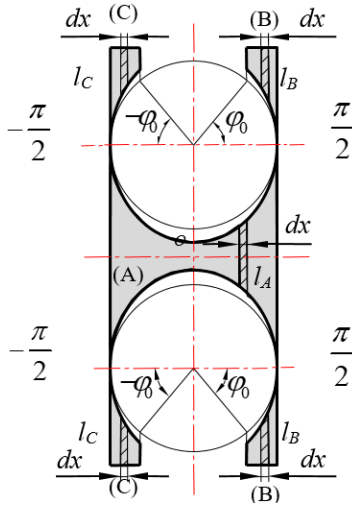


Fig. 4 Partition of the flexure hinge for compliance calculation

The compliance equations can be derived as follow:

1) Angular compliance about y-axis and z-axis:

$$C_{\alpha_z - M_z} = \frac{12b}{EWt^2} \int_{-\pi/2}^{\pi/2} \frac{\cos \phi}{[2a(1 - \cos \phi) + t]^3} d\phi + \frac{3b}{EWn^2} \int_{\phi_0}^{\pi/2} \frac{\cos \phi}{[n + a \cos \phi_0 - a \cos \phi]^3} d\phi, \quad (5a)$$

$$C_{\alpha_y - F_z} = \frac{12b^2}{EWt^3} \int_{-\pi/2}^{\pi/2} \frac{\cos \phi}{2a(1 - \cos \phi) + t} d\phi + \frac{12b^2}{EWt^3} \int_{\phi_0}^{\pi/2} \frac{\cos \phi}{[n + a \cos \phi_0 - a \cos \phi]^3} d\phi, \quad (5b)$$

$$C_{\alpha_z - F_y} = \frac{12b^2}{EWt^2} \int_{-\pi/2}^{\pi/2} \frac{\cos \phi}{[2a(1 - \cos \phi) + t]^3} d\phi + \frac{3b^2}{EWn^2} \int_{\phi_0}^{\pi/2} \frac{\cos \phi}{[n + a \cos \phi_0 - a \cos \phi]^3} d\phi, \quad (5c)$$

$$C_{\alpha_y - M_y} = \frac{12b}{EWt^3} \int_{-\pi/2}^{\pi/2} \frac{\cos \phi}{2a(1 - \cos \phi) + t} d\phi + \frac{12b}{EWt^3} \int_{\phi_0}^{\pi/2} \frac{\cos \phi}{n + a \cos \phi_0 - a \cos \phi} d\phi, \quad (5d)$$

2) Linear compliance along x-, y- and z-axis:

$$C_{x - F_x} = \frac{b}{EW} \int_{-\pi/2}^{\pi/2} \frac{\cos \phi}{2a(1 - \cos \phi) + t} d\phi + \frac{b}{EW} \int_{\phi_0}^{\pi/2} \frac{\cos \phi}{n + a \cos \phi_0 - a \cos \phi} d\phi, \quad (5e)$$

$$C_{z - F_z} = \frac{24b^3}{EW^3} \int_{-\pi/2}^{\pi/2} \frac{\cos \phi}{2a(1 - \cos \phi) + t} d\phi - \frac{12b^3}{EW^3} \int_{-\pi/2}^{\pi/2} \frac{\cos^3 \phi}{2a(1 - \cos \phi) + t} d\phi + \frac{24b^3}{EW^3} \int_{\phi_0}^{\pi/2} \frac{\cos \phi}{n + a \cos \phi_0 - a \cos \phi} d\phi - \frac{b^3}{EW^3} \int_{\phi_0}^{\pi/2} \frac{\cos^3 \phi}{[n + a \cos \phi_0 - a \cos \phi]^3} d\phi, \quad (5f)$$

$$C_{z - F_z} = \frac{24b^3}{EW^3} \int_{-\pi/2}^{\pi/2} \frac{\cos \phi}{2a(1 - \cos \phi) + t} d\phi - \frac{12b^3}{EW^3} \int_{-\pi/2}^{\pi/2} \frac{\cos^3 \phi}{2a(1 - \cos \phi) + t} d\phi + \frac{24b^3}{EW^3} \int_{\phi_0}^{\pi/2} \frac{\cos \phi}{n + a \cos \phi_0 - a \cos \phi} d\phi - \frac{12b^3}{EW^3} \int_{\phi_0}^{\pi/2} \frac{\cos^3 \phi}{n + a \cos \phi_0 - a \cos \phi} d\phi, \quad (5g)$$

$$C_{\alpha_z - F_y} = C_{y - M_z}, \quad (5h)$$

$$C_{\alpha_y - F_z} = C_{z - M_y}, \quad (5i)$$

Among Eqs. (1–9):

$$\phi_0 = \arctan \frac{2mb}{2a\sqrt{4b^2 - m^2}} \quad m \leq 2b,$$

$$n = \frac{H}{2} - \left(a + \frac{t}{2}\right) - \frac{a}{2b} \sqrt{4b^2 - m^2}.$$

From Eqs. (5 a – i), it can be seen that the compliance of U-shape flexure hinge is inversely proportional to the elasticity modulus and the width of the hinge. Moreover, compliance is influenced by the parameters of the notch size. Upon setting the basic structural parameters H and W for the U-shape flexure hinge, its compliance can be expressed as a function of the notch sizes:

$$C = C^f(a, b, m, t). \quad (6)$$

In the following section, the influence of the parameters of notch size on the compliance of the flexure hinges will be analyzed.

3. Influences of the parameters of notch size on the compliance

Without loss of generality, we assume that two of the parameters of notch sizes are variables and the other two parameters are constant. The structural parameters of the flexure joint are given as $H=30$ mm, $W=10$ mm.

When m and t are set as constant, a and b are variables, varying in the ranges of $a \in [4, 5]$ and $b \in [2, 5]$. When a and b are fixed, m and t are variables, varying in the ranges

of $m \in [4, 8]$, $t \in [4, 5]$. Then the relationship between compliance of the U-shape flexure hinge and the parameters of notch sizes a , b and m , t are plotted using Matlab, as shown in Fig. 5, a – g.

Fig. 5, a – g show each compliance of the U-shape flexure hinges with varying a and b . We can observe from the plots characteristics, as described presently.

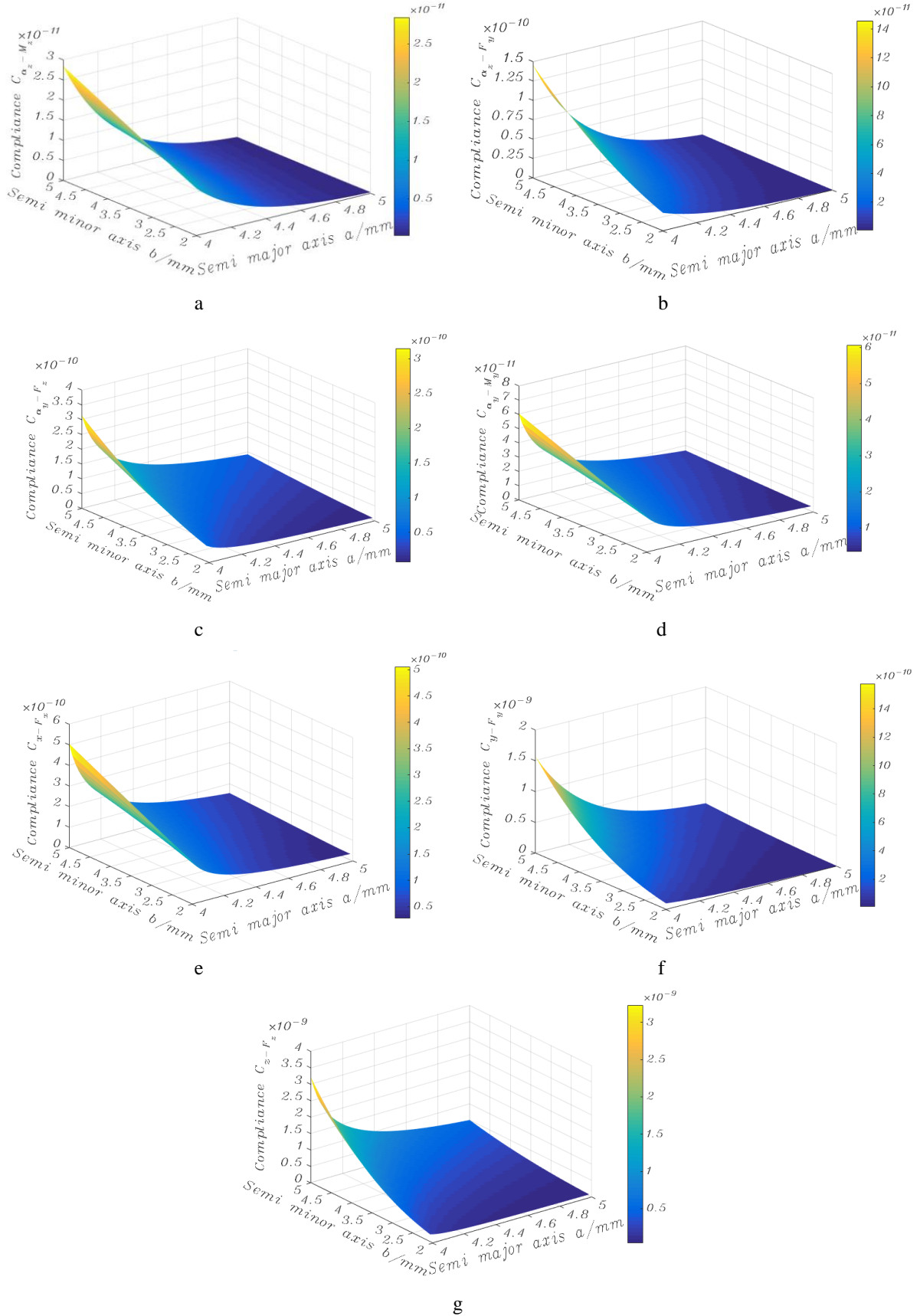


Fig. 5 The influence of parameters a , b on compliance: a – compliance $C_{\alpha_z-M_z}$; b – compliance $C_{\alpha_z-F_y}$; c – compliance $C_{\alpha_x-F_x}$; d – compliance $C_{\alpha_y-M_y}$; e – compliance $C_{\alpha_y-F_z}$; f – compliance C_{y-F_y} ; g – compliance C_{z-F_z}

When a increases, the compliance decreases with a nonlinearity. When b increases, the compliance increases approximate linearly. The influence of b in compliance is more significant. In each compliance, C_{z-F_z} has the maxim-

um value and $C_{a_z-M_z}$ has the minimum value within the value range of a and b . When $a=5$ and $b=2$, each compliance reaches the smallest value.

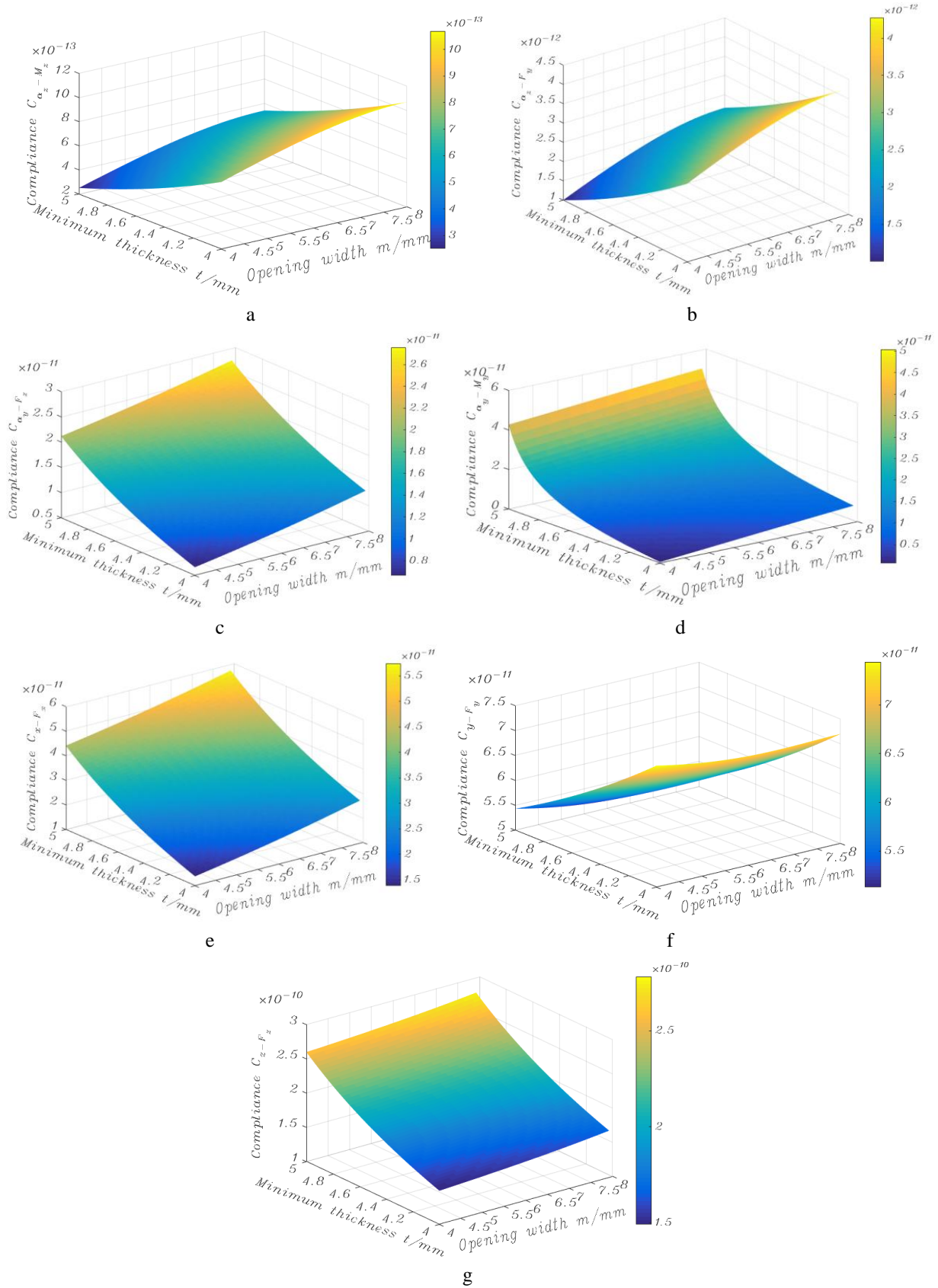


Fig. 6 The influence of parameters m , t on compliance when $a \neq b$: a – compliance $C_{a_z-M_z}$; b – compliance $C_{a_z-F_y}$; c – compliance $C_{a_y-F_z}$; d – compliance $C_{a_y-M_z}$; e – compliance C_{x-F_x} ; f – compliance C_{y-F_y} ; g – compliance C_{z-F_z}

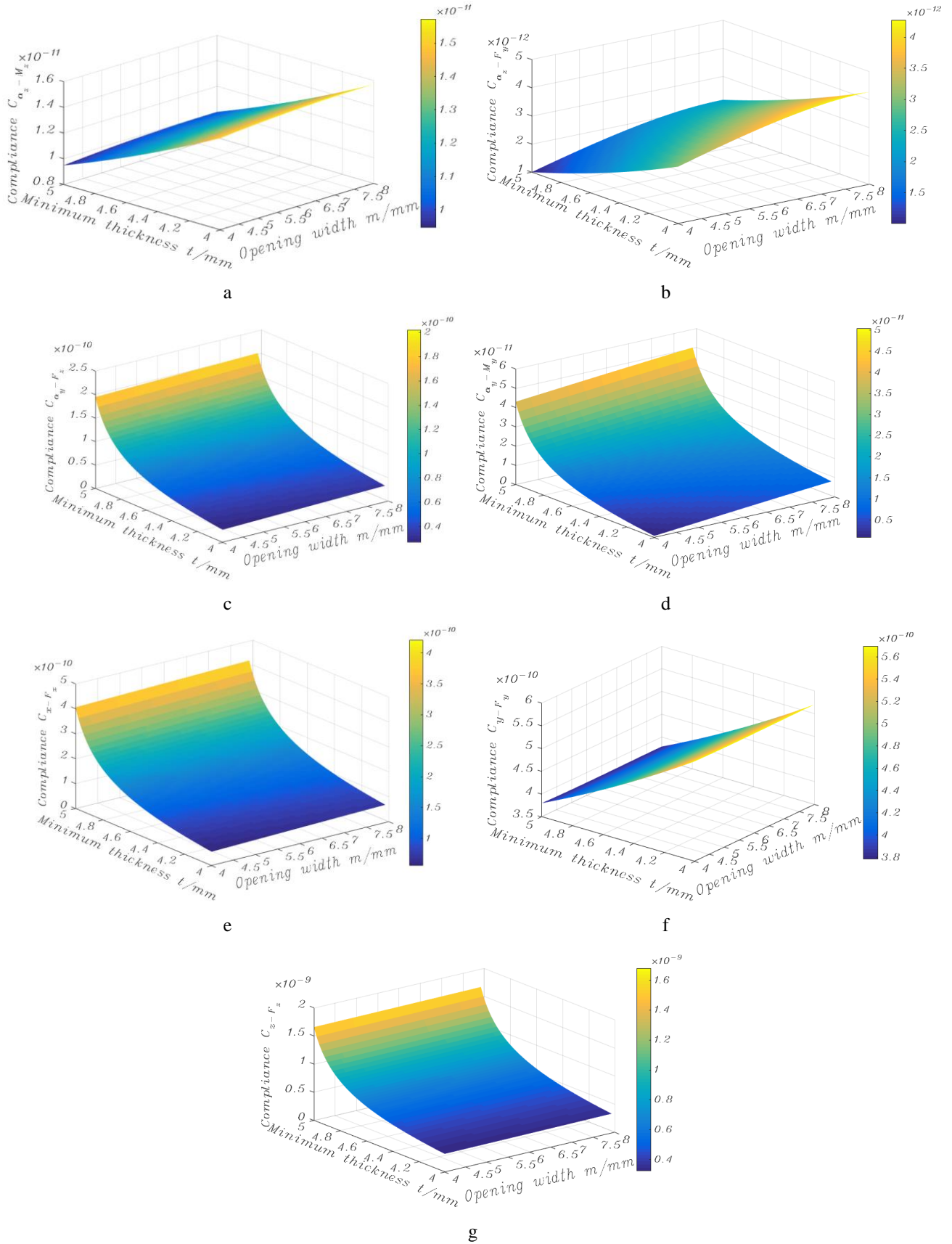


Fig. 7 The influence of parameters m , t on compliance when $a=b$: a – compliance $C_{\alpha_z-M_z}$; b – compliance $C_{\alpha_z-F_y}$; c – compliance $C_{\alpha_y-F_z}$; d – compliance $C_{\alpha_y-M_y}$; e – compliance C_{x-F_x} ; f – compliance C_{y-F_y} ; g – compliance C_{z-F_z}

Fig. 6 shows the compliance of the U-shape flexure hinges varying with respect to m , t when $a \neq b$. Fig. 6 shows that the changes of the compliance of $C_{\alpha_z-M_z}$ (Fig. 6,

a), $C_{\alpha_z-F_y}$ (Fig. 6, b) and C_{y-F_y} (Fig. 6, f) are consistent with increase of m and t , the compliance increases approximately

linearly as m increases, and the compliance decreases approximately linearly as t increases. The change of the compliance of $C_{\alpha_y-F_z}$ (Fig. 6, c), C_{x-F_x} (Fig. 6, e), and C_{z-F_z} (Fig. 6, g) are consistent with the increase of m and t . The compliance increases approximately linearly as m and t increase. The compliance $C_{\alpha_y-M_y}$ (Fig. 6, d) increases nonlinearly as m and t increase. When m and t are the smallest value in the range, the compliance $C_{\alpha_y-F_z}$, $C_{\alpha_y-M_y}$, C_{x-F_x} , and C_{z-F_z} have the smallest value in the range. Fig. 7, a - g show the compliance of the U-shape hinge varying with respect to m and t when $a = b$. Fig. 7 shows that the changes of the compliance of $C_{\alpha_z-M_z}$ (Fig. 7, a), $C_{\alpha_z-F_y}$ (Fig. 7, b) and C_{y-F_y} (Fig. 7, f) are consistent with increase of m and t , the compliance increases approximately linearly as m increases, and the compliance decreases approximately linearly as t increases. The change of the compliance of $C_{\alpha_y-F_z}$ (Fig. 6, c), $C_{\alpha_y-M_y}$ (Fig. 6, d), C_{x-F_x} (Fig. 6, e), and C_{z-F_z} (Fig. 6, g) are consistent with increase of m and t , the compliance increases nonlinearly as m and t increase. When m and t are the smallest in the range, the compliance $C_{\alpha_y-F_z}$, $C_{\alpha_y-M_y}$, C_{x-F_x} , and C_{z-F_z} have the smallest values in the range too.

4. Simulation of fatigue life

When the flexure hinge is applied to the flexible mechanism, the deformation of the mechanism is mainly caused by the large stress of the flexure hinge. The flexible mechanism usually uses piezoelectric ceramics to drive the flexure hinge to produce deformation. The mechanism failure is mainly reflected in the fatigue failure of flexure hinge. Therefore, it is necessary to study the fatigue life of flexure hinge to ensure the reliability of flexible mechanism.

The fatigue failure of flexure hinge under alternating load is generally occurred during the operation. Alternating loads produce alternating stress. Generally, alternating loads are decomposed into a load of constant amplitude and a load of variable amplitude. In this work, a periodic load of constant amplitude 10 N in the X and Y directions is considered. Material is structural steel with Young's Modulus $2e+011$ Pa, Poisson's Ratio 0.3, Bulk Modulus $1.6667e+011$ Pa, Shear Modulus $7.6923e+010$ Pa. The stress and cycle times are shown in Table 1. The fatigue life

of U-shape flexure hinge was analysed by ANSYS simulation, and a series of fatigue life of U-shape flexure hinge with different notch size parameters were obtained, as listed in Table 2.

The main notch parameters of the U-shape flexure hinge are a , b , m , t . There are thirty models in three groups. The notch parameters are as follows:

$a=8$, $b=8$, $m=14$, while t is variable;

$a=6$, $b=5$, $t=6$, while m is variable;

$t=1$, $m=3$, while a , b are variables.

The finite element model of the U-shape flexure hinge is built in the workbench. The left end is fixed, the right end loading (axial force, lateral force, bending moment), insert the fatigue analysis module Fatigue Tool and set the correction coefficient of fatigue analysis. The fatigue life cloud figure of the U-shape flexure hinge is shown in Fig. 8. Fatigue life is obtained, as shown in Table 2.

Curve fitting is carried out in Matlab. The influence curve of the notch parameter on the fatigue life of flexure hinge is obtained, as shown in Fig. 9, a - c.

Table 1

Stresses and cycles

Alternating stress, Pa	Cycles
3.999e+009	10
2.827e+009	20
1.896e+009	50
1.413e+009	100
1.069e+009	200
4.41e+008	2000
2.62e+008	10000
2.14e+008	20000
1.38e+008	1.e+005
1.14e+008	2.e+005
8.62e+007	1.e+006

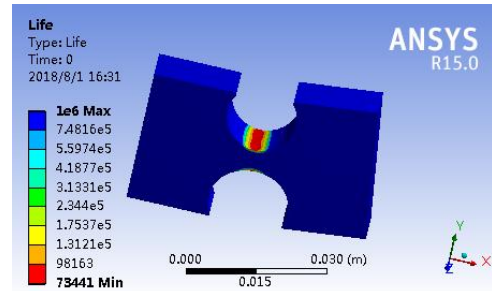


Fig. 8 Fatigue life cloud figure of U-shape flexure hinge with parameters $a=8$, $b=8$, $m=14$, $t=5$

Table 2

Fatigue life of U-shape flexure hinge under different incision parameters

$a=8, b=8, m=14$	$t=1$	$t=2$	$t=3$	$t=4$	$t=5$
$N(\log N)$	13.803 (1.14)	599.73 (2.778)	2706.6 (3.4324)	13090 (4.1169)	73441 (4.8659)
$a=8, b=8, m=14$	$t=6$	$t=7$	$t=8$	$t=9$	$t=10$
$N(\log N)$	186060 (5.2697)	15545 (4.1916)	36157 (4.5582)	64214 (4.8076)	85065 (4.9298)
$a=6, b=5, t=6$	$m=3.5$	$m=4$	$m=4.5$	$m=5$	$m=5.5$
$N(\log N)$	146010 (5.1644)	145230 (5.1621)	146750 (5.1666)	145460 (5.1627)	147840 (5.1698)
$a=6, b=5, t=6$	$m=6$	$m=6.5$	$m=7$	$m=7.5$	$m=8$
$N(\log N)$	145190 (5.1619)	145470 (5.1628)	147800 (5.1697)	147230 (5.168)	147300 (5.1682)
$t=1, m=3$	$a=2.5, b=1.5$	$a=3, b=2$	$a=3.5, b=2.5$	$a=4, b=3$	$a=4.5, b=3.5$
$N(\log N)$	17.16 (1.2345)	16.537 (1.2185)	13.775 (1.1391)	13.861 (1.1418)	15.006 (1.1763)
$t=1, m=3$	$a=5, b=4$	$a=5.5, b=4.5$	$a=6, b=5$	$a=6.5, b=5.5$	$a=7, b=6$
$N(\log N)$	14.77 (1.1694)	14.633 (1.1653)	14.042 (1.1474)	13.975 (1.1454)	13.811 (1.1402)

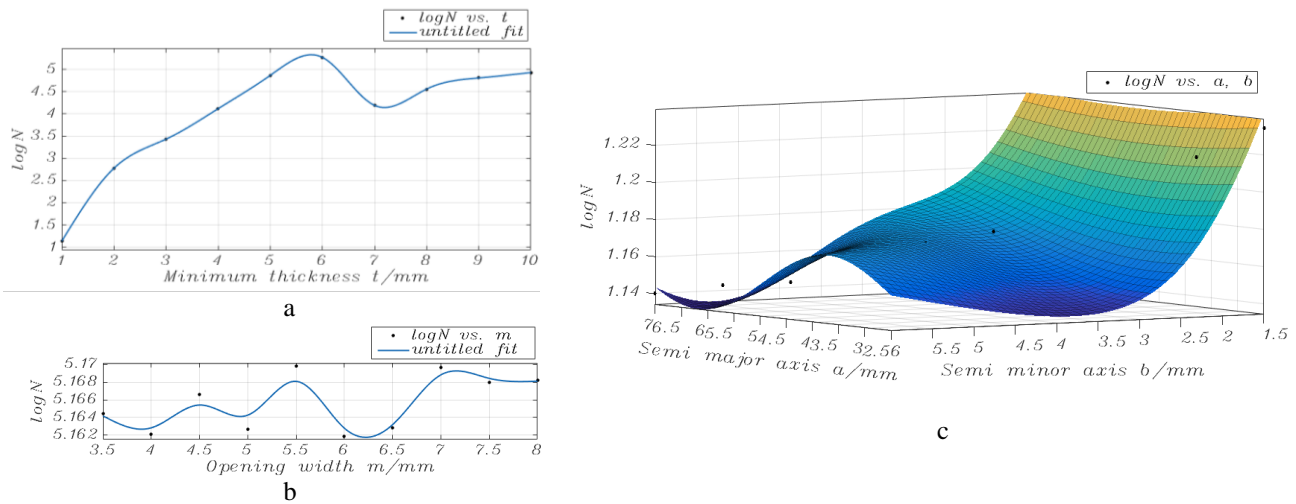


Fig. 9 The influence of parameters on fatigue life: a – the influence of thickness, b – the influence of m , c – the influence of a, b

5 Comparison of the fatigue life and stress of U-shape flexure

U-shape flexure hinges and circular arc flexure hinge with the same center thickness $t=6$ are selected for analysis and comparison. The notch parameters of circular-arc-shaped flexure hinge are $r=12, m=24, t=6$; The model is established in ANSYS to analyze the fatigue life and stress. The analysis results of circular-arc-shaped flexure hinge are shown in Figs.10, a-b. The notch parameters and

analysis results of four structures U-shape flexure hinges are shown in Table 3.

The results show that the fatigue life of the three structures of U-shape flexure hinges (U-shape with a semi-circle is tangent to a line segment, U-shape with a semi-ellipse is tangent to the line segment, U-shape with an arc intersects the line segment) is higher than that of circular arc flexure hinge, while the stress of three structures of U-shape flexure hinges is less than that of circular arc flexure hinge. Therefore, the three structures of U-shape flexure hinges are more reliable than the circular arc flexure hinge.

Table 3

Fatigue life and stress of U-shape flexure hinges

Semicircle is tangent to a line segment notch	$a=b=10$ $m=20, t=6$	$a=b=9$ $m=18, t=6$	$a=b=8$ $m=16, t=6$	$a=b=7$ $m=14, t=6$	$a=b=6$ $m=12, t=6$
Fatigue life	1.9397e5	1.9042e5	1.8603e5	1.7897e5	1.707e5
Stress	4.8043e6	4.8543e6	4.9154e6	5.005e6	5.1129e6
Semi-ellipse is tangent to the line segment notch	$a=11.5, b=10$ $m=20, t=6$	$a=11, b=10$ $m=18, t=6$	$a=11, b=10$ $m=20, t=6$	$a=10, b=8$ $m=16, t=6$	$a=9, b=8$ $m=16, t=6$
Fatigue life	1.8899e5	1.8297e5	1.9083e5	1.7569e5	1.7987e5
Stress	4.87e6	4.9554e6	4.8474e6	5.0468e6	4.9912e6
Arc intersects the line segment notch	$a=b=9$ $m=17, t=6$	$a=b=8$ $m=14, t=6$	$a=b=7$ $m=10, t=6$	$a=b=6.5$ $m=10, t=6$	$a=b=6$ $m=10, t=6$
Fatigue life	1.9042e5	1.8606e5	1.7898e5	1.7638e5	1.7069e5
Stress	4.8543e6	4.9152e6	5.0048e6	5.0413e6	5.1131e6
Elliptical arc intersects the line segment notch	$a=9, b=7$ $m=13.5, t=6$	$a=8, b=7$ $m=13, t=6$	$a=8, b=6$ $m=11, t=6$	$a=7, b=6$ $m=11, t=6$	$a=6, b=5$ $m=9, t=6$
Fatigue life	1.655e5	1.7192e5	1.5298e5	1.6186e5	1.4747e5
Stress	5.1749e6	5.0946e6	5.3338e6	5.2222e6	5.4046e6

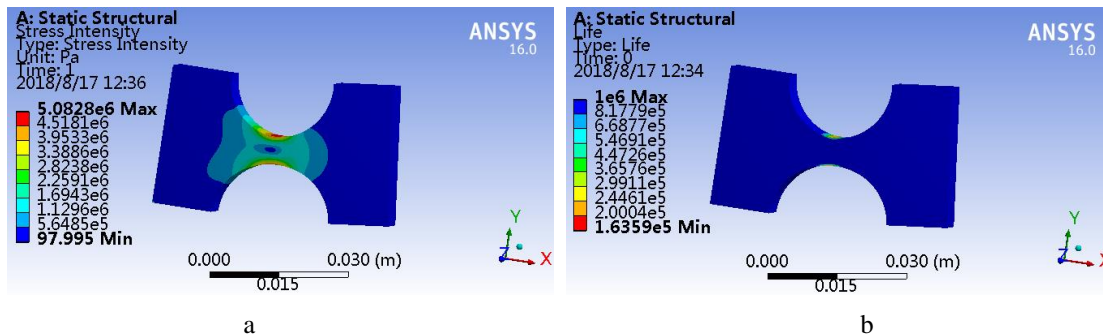


Fig. 10 Analysis results of circular-arc-shaped flexure hinge: a – the stress distribution, b – the fatigue life cloud figure

6. Conclusions

The compliance equations for the U-shape flexure hinges have been derived using the Castigliano's second theorem. The influence of structure parameters on the compliance of U-shape flexure hinges is analyzed on the basis of establishing the model. The results indicate that the compliance of U-shape flexure hinge have different trends with notch parameters change, and have different sensitivity to the change of the notch parameters within the given range. The influence of notch parameters b and t on compliance is more obvious than that of notch parameters a and m .

The fatigue life is analyzed by changing the U-shape flexure hinge notch parameter. The results show that the fatigue life of flexure hinge increases gradually with the increasing of flexure hinge center thickness t . The fatigue life of flexure hinge increases with the increasing of hinge notch width m . With the increasing of the major axis of the ellipse a and semi minor axis of the ellipse b , the fatigue life of flexure hinge fluctuates locally, the general trend is a gradual decrease. There are three structures of the U-shape flexure hinges that are more reliable than the circular arc flexure hinge, U-shape with a semi-circle is tangent to a line segment, U-shape with a semi-ellipse is tangent to the line segment, and U-shape with an arc intersects the line segment.

In summary, compliance and fatigue life of the U-shape flexure hinges is related to material properties and structure parameters, among which the influence of the notch parameters on the compliance and fatigue life is more obvious.

Acknowledgement

This research was funded by the key research and development project of Shanxi province (Grant Nos. 201803D421027, 201803D421028), the foundation of Shanxi key laboratory of advanced manufacturing technology (Grant No. XJZZ201702), and the natural science foundation of Shanxi province (Grant No. 015011060).

References

1. Yu, J. J.; Pei, X.; Bi, S. S.; Zong, G. H.; Zhang, X. M. 2010. State-of-arts of design method for flexure mechanisms, *Journal of Mechanical Engineering* 46(13): 2-13 (in Chinese).
2. Yu, J. J.; Hao, G. B.; Chen, G. M.; Bi, S. S. 2015. State-of-art of compliant mechanisms and their applications, *Journal of Mechanical Engineering* 51(13): 53-68 (in Chinese).
3. Wu, J. W.; Zhang, Y.; Cai, S.; Cui, J. W. 2018. Modeling and analysis of conical-shaped notch flexure hinges based on NURBS, *Mechanism and Machine Theory* 128: 560-568.
4. Yang, M.; Du, Z. J.; Dong, W. 2016. Modeling and analysis of planar symmetric superelastic flexure hinges, *Precision Engineering* 46: 177-183.
5. Chen, G. M.; Howell, L. L. 2009. Two general solutions of torsional compliance for variable rectangular cross-section hinges in compliant mechanisms, *Precision Engineering* 33(3): 268-274.
6. Tian, Y.; Shirinzadeh, B.; Zhang, D.; Zhong, Y. 2010. Three flexure hinges for compliant mechanism designs based on dimension less graph analysis, *Precision Engineering* 34(1): 92-100.
7. Friedrich, R.; Lammering, R.; Rösner, M. 2014. On the modeling of flexure hinge mechanisms with finite beam elements of variable cross section, *Precision Engineering* 38(4): 915-920.
8. Dirksen, F.; Anselmann, M.; Zohdi, T. I.; Lammering, R. 2013. Incorporation of flexural hinge fatigue-life cycle criteria into the topological design of compliant small-scale devices, *Precision Engineering* 37(3): 531-541.
9. Wang, X. J.; Liu, C. L.; Gu, J. J.; Zhang, W. J. 2015. A parametric model for rotational compliance of a cracked right circular flexure hinge, *International Journal of Mechanical Sciences* 94-95: 168-173.
10. Li, L. J.; Zhang, D.; Guo, S.; Qu, H. B. 2017. A generic compliance modeling method for two-axis elliptical-arc-filletted flexure hinges, *Sensors* 17(9): 21-54.
11. Wu, J. W.; Cai, S.; Cui, J. W.; Tan, J. B. 2015. A generalized analytical compliance model for cartwheel flexure hinges, *Review of Scientific Instruments* 86: 105003(1-11).
12. Tian, Y.; Shirinzadeh, B.; Zhang, D. Closed-form compliance equations of filletted V-shaped flexure hinges for compliant mechanism design, *Precision Engineering* 34(3): 408-418.
13. Chen, G. 2014. Generalized equations for estimating stress concentration factors of various notch flexure hinges, *Journal of Mechanical Design* 136(3): 252-261.
14. Xu, N.; Dai, M.; Zhou, X. Q. 2017. Analysis and design of symmetric notch flexure hinges, *Advances in Mechanical Engineering* 9(11): 1-12.
15. Li, L. J.; Zhang, D.; Guo, S.; Qu, H. B. 2019. Design, modeling, and analysis of hybrid flexure hinges, *Mechanism and Machine Theory* 131: 300-316.
16. Wang, X. J.; Liu, C. L.; Gu, J. J.; Zhang, W. J. 2015. A parametric model for rotational compliance of a cracked right circular flexure hinge, *International Journal of Mechanical Sciences* 94-95: 168-173.
17. Li, Q.; Pan, C. Y.; Xu, X. J. 2013. Closed-form compliance equations for power-function-shaped flexure hinge based on unit-load method, *Precision Engineering* 37: 135-145.
18. Meng, Q.; Li, Y.; Xu, J. 2013. New empirical stiffness equations for corner-filletted flexure hinges, *Mechanical Sciences* 4(2): 345-356.
19. Li, T. M.; Zhang, J. L.; Jiang, Y. 2015. Derivation of empirical compliance equations for circular flexure hinge considering the effect of stress concentration, *International Journal of Precision Engineering and Manufacturing* 16(8): 1735-1743.
20. Lobontiu, N.; Paine, J. S. N.; Garcia, E.; Goldfarb, M. 2002. Design of symmetric conic-section flexure hinges based on closed-form compliance equations, *Mechanism and Machine Theory* 37: 477-498.

J.J. Liang, R.Q. Li, S.P. Bai, Q. Li, F.P. Ning, S.H. Kang

COMPLIANCE AND FATIGUE LIFE ANALYSIS OF U-SHAPE FLEXURE HINGE

S u m m a r y

This paper establishes four models of U-shape flexure hinges with different notch shapes and structure parameters, and presents the close-form compliance equations for the four structure types of U-shape flexure hinges. The compliance of the flexure hinges is developed based on the Castiglione's second theorem and calculus theory. A relationship between compliances and structure parameters is deduced using the models. The influences of the notch structure parameters on the compliance of the flexure hinges are investigated. Moreover, fatigue life of U-shape flexure

hinges is studied by finite element analysis, the results show that the fatigue life of flexure hinge increases gradually with the increasing of flexure hinge center thickness t and hinge notch width m . With the increasing of the major axis of the ellipse a and semi minor axis of the ellipse b , the fatigue life of flexure hinge fluctuates locally, the general trend is a gradual decrease. The stress and fatigue life of U-shape flexure hinges and arc flexure hinge are compared. The results show that the reliability of U-shape flexure hinge is higher than that of circular arc flexure hinge.

Keywords: compliance, fatigue life, reliability, U-shape flexure hinge.

Received February 04, 2019

Accepted November 21, 2019